

# Benzamides and benzamidines as specific inhibitors of epidermal growth factor receptor and v-Src protein tyrosine kinases

Toru Asano,<sup>b</sup> Tomohiro Yoshikawa,<sup>a</sup> Taikou Usui,<sup>a</sup> Hiroshi Yamamoto,<sup>a</sup>  
Yoshinori Yamamoto,<sup>b</sup> Yoshimasa Uehara<sup>c</sup> and Hiroyuki Nakamura<sup>a,\*</sup>

<sup>a</sup>Department of Chemistry, Faculty of Science, Gakushuin University, Mejiro, Toshima-ku, Tokyo 171-8588, Japan

<sup>b</sup>Department of Chemistry, Graduate School of Science, Tohoku University, Sendai 980-8588, Japan

<sup>c</sup>Department of Bioactive Molecules, National Institute of Infectious Diseases, Tokyo 162-8640, Japan

Received 21 March 2004; revised 26 April 2004; accepted 26 April 2004

Available online 18 May 2004

**Abstract**—The benzamides **1** and the benzamidines **2** as well as the cyclic benzamidines **3** were designed and synthesized as the mimics of 4-anilinoquinazolines for an inhibitor of EGFR tyrosine kinase. The specific inhibitions of EGFR tyrosine kinase were observed in the benzamides **1c** and **1d**, and the benzamidine **2a**, whereas the specific inhibitions of v-Src kinase were observed in the benzamide **1j** and the benzamidine **2d** at a 10 µg/mL concentration of compounds. The cyclic benzamidines **3a** and **3b** showed potent kinase inhibition of EGFR at a 1.0 µg/mL concentration. According to the docking simulation using the X-ray structure of EGFR kinase domain in complex with erlotinib, the LigScore2 scoring function value of erlotinib was calculated as 5.61, whereas that of the benzamide **1c** was 5.05. In a similar manner, the LigScore2 value of the cyclic benzamidine **3a** was calculated as 5.10.  
© 2004 Elsevier Ltd. All rights reserved.

## 1. Introduction

The epidermal growth factor receptor (EGFR) protein tyrosine kinase (PTK) is one of the important kinases that play a fundamental role in signal transduction pathways. EGFR and its ligands (EGF, TGF- $\alpha$ ) have been implicated in numerous tumors of epithelial origin<sup>1,2</sup> and proliferative disorders of the epidermis such as psoriasis.<sup>3</sup> Therefore, the design of inhibitors toward EGFR-PTK is an attractive approach for the development of new therapeutic agents.<sup>4–7</sup>

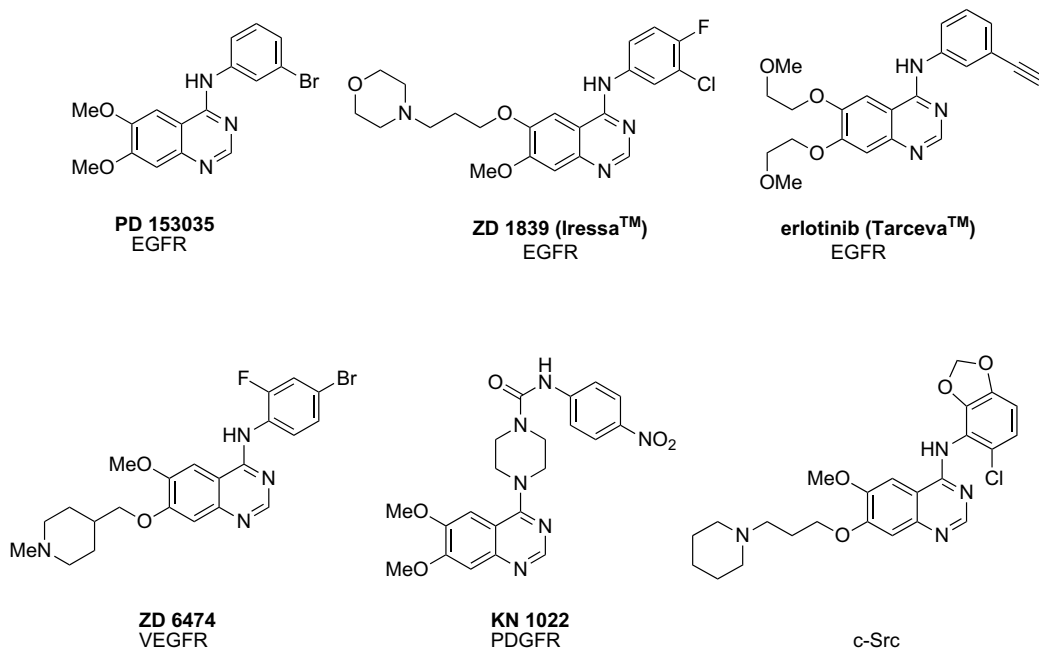
In 1994, Fry et al. discovered that the 4-anilinoquinazoline (PD 153035) possess a specific inhibitory activity toward EGFR tyrosine kinase.<sup>8</sup> Various 4-anilinoquinazoline derivatives have been synthesized so far based upon the structure of PD 153035,<sup>9–14</sup> and ZD1839 (Iressa™)<sup>15</sup> was found to be effective for non-small cell lung cancer and recently approved for the clinical use in Japan. Furthermore, 4-anilinoquinazoline derivatives (ZD 6474, KN 1022, etc.) have been investigated as

potent inhibitors of vascular endothelial growth factor receptor (VEGFR),<sup>16,17</sup> platelet-derived growth factor receptor (PDGFR),<sup>18</sup> c-Src,<sup>19,20</sup> and other kinases.<sup>21</sup>

According to the crystal structure of the EGFR kinase domain and in complex with erlotinib, which was recently reported by Eigenbrot and co-workers, the interplanar angle of quinazoline and aniline rings in erlotinib is 42° and a hydrogen bonding between the Met-769 amide nitrogen of the kinase domain and the nitrogen (N1) of the quinazoline ring has been observed. The other quinazoline nitrogen (N3) forms a hydrogen bonding to the Thr-766 side chain through a water molecule.<sup>22</sup> We thought that the flexibility of the quinazoline framework would be effective for the interaction between the kinase domain and inhibitors. In this article, we designed the benzamides **1** and the benzamidines **2** as the mimics of 4-anilinoquinazolines and expected a pseudocycle formation through intramolecular hydrogen bonding in the molecules.<sup>23–26</sup> The benzamides **1** and the benzamidines **2** as well as the cyclic benzamidines **3** were synthesized and examined their biological properties:<sup>27</sup> cytotoxicity and inhibitory activity toward various tyrosine kinases. Furthermore, docking simulations of the benzamides **1**, the benzamidines **2**, and the cyclic benzamidines **3** were

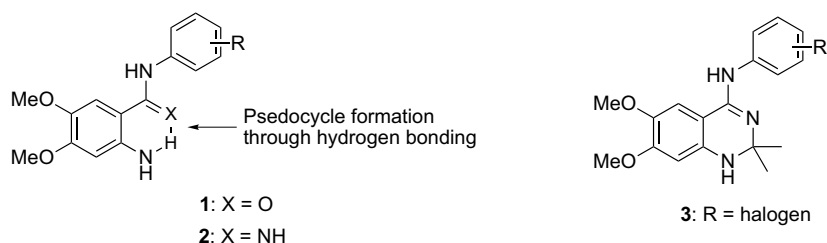
**Keywords:** EGFR; Tyrosine kinase; Inhibitor.

\* Corresponding author. Tel.: +81-339860221; fax: +81-359921029; e-mail: [hiroyuki.nakamura@gakushuin.ac.jp](mailto:hiroyuki.nakamura@gakushuin.ac.jp)



demonstrated using the X-ray structure of EGFR kinase domain in complex with erlotinib (Tarceva™) and evaluated their structure–activity relationship.

anthranilic acid **4** by two different pathways as shown in Scheme 2. The anthranilamides **1a** was synthesized from **4** through the formation of the carbamate **5**.<sup>30</sup> The ring



## 2. Result and discussion

### 2.1. Chemistry

We first examined the synthesis of the 4,5-dimethoxyanthranilamides **1** from commercially available 2-amino-4,5-dimethoxybenzonitrile as shown in Scheme 1.<sup>28,29</sup> The progress of the reaction was confirmed by the consumption of 2-amino-4,5-dimethoxybenzonitrile on TLC. Although the reaction proceeded, separation of **1c** from the reaction mixture containing aluminum complexes was not easy due to high polarity of the product.

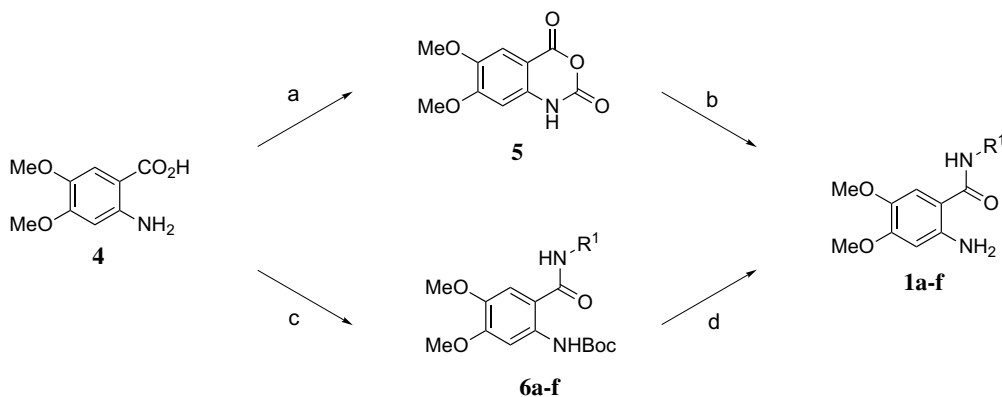
We next examined the synthesis of the 4,5-dimethoxyanthranilamides **1a–f** from 2-amino-4,5-dimethoxy-



**Scheme 1.** Reagents and conditions: (a) 3-bromoaniline, AlCl<sub>3</sub>, neat, 180 °C.

opening of the carbamate **5**, which was derived from **4** with ethyl chloroformate,<sup>31</sup> with cyclohexylamine at 110 °C afforded the anthranilamide **1a** in 67% yield, however, the reaction with 3-chloro-4-fluoroaniline afforded the anthranilamide **1f** in a very low yield. Alternatively, the synthetic route using the EDCI-promoted amide formation was examined. The amidation of the *N*-Boc protected benzoic acid of **4** with cyclohexylamine gave **6a** in 78% yield, and the deprotection of the Boc group with trifluoroacetic acid afforded the anthranilamide **1a**, quantitatively. Surprisingly, the EDCI-promoted amidation of the *N*-Boc protected benzoic acid of **4** with 3-chloro-4-fluoroaniline proceeded smoothly to afford **6f** in 70% yield. The deprotection of the Boc group afforded the anthranilamide **1f**, quantitatively. Other amines (R<sup>1</sup>NH<sub>2</sub>) such as 1-phenylethylamine, 3-bromoaniline, 3-trifluoroaniline, and 3-methoxyaniline, also underwent the EDCI-promoted amidation to afford the amides **6b–e**, respectively, and the deprotection of the Boc group with trifluoroacetic acid afforded the anthranilamides **1b–e** in 63–>99% yields.

Although several attempts have been made for the synthesis of the 2-pyridylamino-4,5-dimethoxyanthranilamides **1g–i**, which contain pyridyl moieties at the R<sup>1</sup>



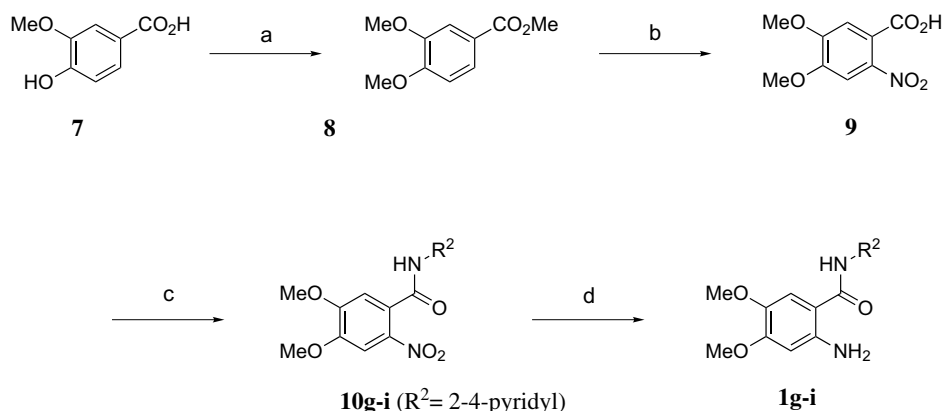
**Scheme 2.** Reagents and conditions: (a) i. ethyl chloroformate, THF, reflux; ii.  $\text{PBr}_3$ ,  $\text{Et}_2\text{O}$ , reflux; (b)  $\text{R}_1\text{NH}_2$ , DMF,  $100^\circ\text{C}$ ; (c) i.  $(\text{Boc})_2\text{O}$ , NaOH,  $\text{H}_2\text{O}$ ; ii.  $\text{R}_1\text{NH}_2$ , EDCI, HOBt, DMF; (d) TFA,  $\text{CH}_2\text{Cl}_2$ .

group, in a similar manner, the amide bond formations did not take place, probably due to the weak nucleophilicity of pyridylamines in comparison with cyclohexyl and phenethyl amines, and anilines. We succeeded in the synthesis of the 2-pyridylamino-4,5-dimethoxyanthranilamides **1g–i** from vanillic acid **7** through the amide formation of pyridyl amines with the acid halide as shown in Scheme 3. The vanillic acid **7** was converted to the methyl ester in MeOH at reflux and then methylated with iodomethane in acetone to give methyl 3,4-dimethoxybenzoate **8**. Selective nitration at the C6 position of **8** with 70% nitric acid in acetic acid at  $50\text{--}60^\circ\text{C}$  followed by hydrolysis of a methyl ester afforded the 2-nitrobenzoic acid **9**. The 2-nitrobenzoic acid **9** was treated with thionyl chloride in refluxing  $\text{CH}_2\text{Cl}_2$  to convert the corresponding acid chloride, which underwent the amide bond formation with pyridylamines to give the 2-nitrobenzylamides **10g–i**. The reduction of **10g–i** with tin(II) chloride in MeOH afforded the 2-pyridylamino-4,5-dimethoxyanthranilamides **1g–i** in good yields.<sup>32</sup>

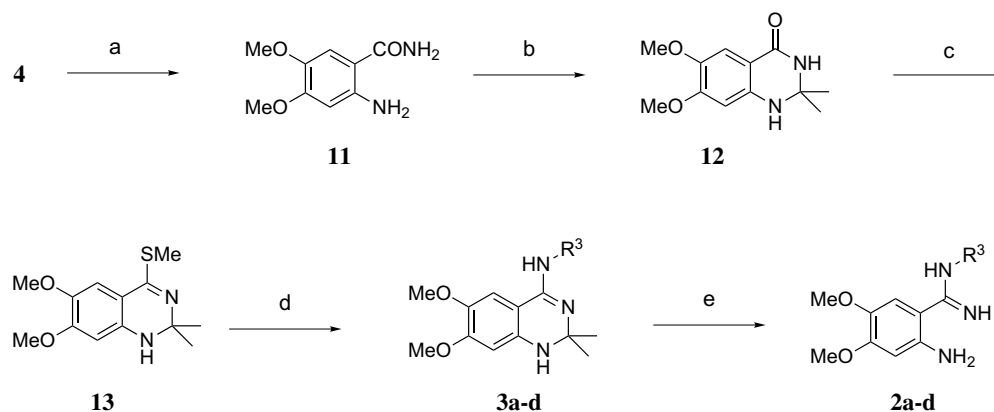
As illustrated in Scheme 4, the 2-amino-4,5-dimethoxyphenylamidines **2a–d** were synthesized from 4,5-dimethoxyanthranilic acid **4** by six steps.<sup>33</sup> The amidation reaction of **4** with ammonia proceeded in the presence of

DCC and HOBt to give 4,5-dimethoxyanthranilamide **11**, which was converted to the protected amide **12**. The treatment of **12** with Lawesson's reagent at  $80^\circ\text{C}$  followed by methylation with iodomethane afforded the thioamidate **13**. The nucleophilic substitution of the methanethiol group in **13** by 3-bromoaniline in MeOH resulted in the formation of the undesired product, 4,6,7-trimethoxy-2,2-dimethyl-1,2-dihydro-quinazoline, which was generated by the nucleophilic attack of methanol instead of 3-bromoaniline. The substitution reactions of the thioamidate **13** were also examined in the different solvents, such as THF, DMF, and MeCN, however, **12**, which was obtained by hydrolysis of **13**, was observed in all cases. After several attempts, we found that the substitution reactions of the thioamidate **13** by anilines proceeded without any solvents at  $110^\circ\text{C}$  to give the corresponding cyclic benzamidines **3a–d**. The deprotection of **3a–d** was carried out under the acidic condition to give the 2-amino-4,5-dimethoxyphenylamidines **2a–d**.

We next designed 2,3,4-trimethoxyanthranilamide **1j** as the mimics of 4-anilinoquinazoline, where the rigid conformation would be expected through the double intramolecular hydrogen bondings: one would be formed between an oxygen of the 2-methoxy group and



**Scheme 3.** Reagents and conditions: (a) i. concd  $\text{H}_2\text{SO}_4$ , MeOH, reflux; ii. MeI,  $\text{K}_2\text{CO}_3$ , acetone, reflux; (b) i.  $\text{HNO}_3$ , AcOH,  $50\text{--}60^\circ\text{C}$ ; ii. NaOH, THF; (c) i.  $\text{SOCl}_2$ ,  $\text{CH}_2\text{Cl}_2$ , reflux; ii. pyridylamine,  $\text{CH}_2\text{Cl}_2$ ; (d)  $\text{SnCl}_2$ , MeOH.



**Scheme 4.** Reagents and conditions: (a)  $\text{NH}_3$ , DCC, HOBT, THF; (b) acetone, *p*-TsOH, reflux; (c) i. Lawesson's reagent, 80 °C; ii. MeI; (d) amine, neat, 110 °C; (e) HCl, reflux.

a hydrogen of the amide group, and the other would be formed between a hydrogen of amino group and a carbonyl oxygen, as shown in Figure 1. The synthesis of 2,3,4-trimethoxyantranilamide **1j** was accomplished from 2,3,4-trimethoxyantranilic acid **14** as shown in Scheme 5. The nitration of 2,3,4-trimethoxy benzoic acid **14** with 70% nitric acid at 0 °C afforded the corresponding 6-nitrobenzoic acid **15**.<sup>34</sup> The 6-nitrobenzoic acid **15** was treated with thionyl chloride to generate the acid chloride, which underwent the amide formation with 3-bromoaniline to give the 6-nitrobenzamide **16**. The hydrogenation of **16** in the presence of Pd/C in

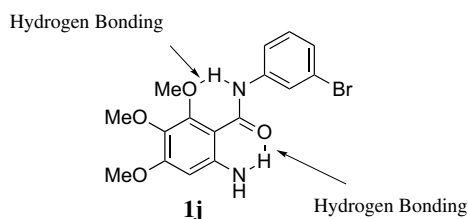
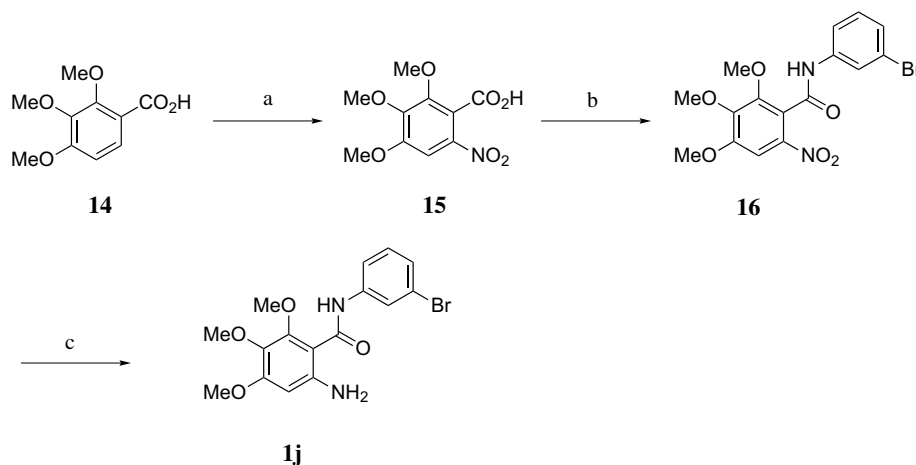


**Figure 1.** A rigid conformation through intramolecular double hydrogen bondings.



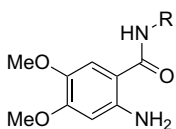
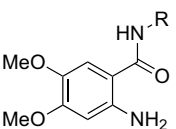
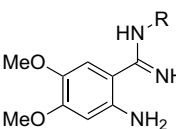
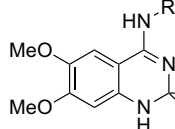
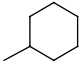
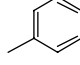
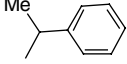
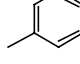
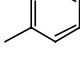
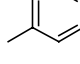
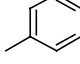
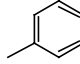
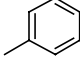
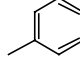
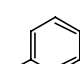
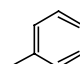
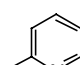
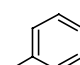
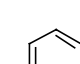
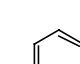
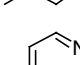
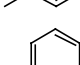
**Scheme 5.** Reagents and conditions: (a) 70%  $\text{HNO}_3$ , 0 °C; (b) i.  $\text{SOCl}_2$ ,  $\text{CH}_2\text{Cl}_2$ , reflux; ii. 3-bromoaniline; (c)  $\text{H}_2$ , Pd/C, MeOH.

MeOH afforded 2,3,4-trimethoxyantranilamide **1j**, quantitatively.

## 2.2. Biological evaluation

The cytotoxicity of the benzamides **1a–j**, the benzamidines **2a–d**, and **3a–d** toward A431<sup>35</sup> human epidermoid carcinoma cells was determined. The concentration of compounds, which exhibited the 50% cell growth inhibition, is shown as an  $\text{IC}_{50}$  value in Table 1. The benzamides **1c–e** and **1j**, which have a substituent at the *meta* position on the aniline group in the molecules, exhibited the cell growth inhibition and the  $\text{IC}_{50}$  values are 0.34, 0.47, 0.20, and 0.92 mM, respectively, although the 50% cell growth inhibition was not observed at a 1.0 mM concentration of the benzamides **1a–b** and **1f–i**. The benzamidines **2a–d** exhibited the similar cell growth inhibitions as the corresponding benzamides and the  $\text{IC}_{50}$  values are 0.20–0.46 mM. Interestingly, the cyclic benzamidines **3a–d** exhibited relatively higher cell growth inhibitions in comparison with the corresponding benzamidines **2a–d** and the  $\text{IC}_{50}$  values are 0.09–0.32 mM.

**Table 1.** Cytotoxicity of the benzamides **1a–j**, and the benzamidines **2a–d** and **3a–d** toward A431 cells

											
<b>1</b>	R	IC <sub>50</sub> (mM) <sup>a</sup>	<b>1j</b>	R	IC <sub>30</sub> (mM)	<b>2</b>	R	IC <sub>30</sub> (mM)	<b>3</b>	R	IC <sub>30</sub> (mM)
<b>1a</b>		>1		<b>2a</b>				0.30			
<b>1b</b>		>1		<b>2b</b>				0.46			
<b>1c</b>		0.34		<b>2c</b>				0.34			
<b>1d</b>		0.47		<b>2d</b>				0.20			
<b>1e</b>		0.20		<b>3a</b>				0.13			
<b>1f</b>		>1		<b>3b</b>				0.20			
<b>1g</b>		>1		<b>3c</b>				0.32			
<b>1h</b>		>1		<b>3d</b>				0.09			
<b>1i</b>		>1									
<b>1j</b>		0.92									

<sup>a</sup> An IC<sub>50</sub> of >1 indicates that no curve was noted in the dose response up to 1 mM.

The benzamides **1a–j**, the benzamidines **2a–d** and **3a–d**, were tested for the inhibitory activity of EGF-stimulated EGFR tyrosine kinase phosphorylation according to assay conditions described in detail in the literature.<sup>36</sup> AG1478 and ZD1839 were also tested as a control inhibitor for the kinase assay. As a preliminary experiment, the inhibition assay of EGFR tyrosine kinase was carried out at a 10 µg/mL concentration of compounds as shown in Figure 2. The maximum phosphorylation activity to the peptide substrate by the EGF-stimulated EGFR tyrosine kinase is plotted as 100% activity after reduction of the kinase activity without stimulated by EGF. Among the compounds synthesized, the cyclic benzamidines **3a** and **3b** exhibited inhibitory activities higher than 50% at a 10 µg/mL concentration, therefore the kinase assay was carried out at lower concentrations (1.0 and 0.1 µg/mL). AG1478 and ZD1839, which have been reported to be potent inhibitors of EGFR tyrosine kinase,<sup>5–7</sup> showed high inhibition of the kinase activity: The phosphorylation activities were 10% and 35% at a

0.1 µg/mL concentration of compounds, respectively. Although the inhibitory activity of the compounds **1a–j**, **3c**, and **2a–d** did not show significant kinase inhibition at a 10 µg/mL concentration, the only pseudocycle **1d**, which has trifluoromethyl group at a *meta* position on the aniline moiety, exhibited a high inhibitory activity at a 10 µg/mL concentration. However, the pseudocycle **1d** did not show the expected kinase inhibition at a 1.0 µg/mL concentration. Interestingly, the cyclic benzamidines **3a** and **3b**, which have the cyclic framework by conjunction with a ketal formation in the molecule, showed high inhibitions at 10 and 1.0 µg/mL concentrations.

Inhibition specificity of the compounds **1c**, **1d**, **1j**, **2a**, **2d**, and **3a** was investigated semi-quantitatively using PKA, PKC, v-Src, eEF2K, and Flt-1 (Table 2).<sup>37–43</sup> The indications ++, +, and – mean >80%, 50–80%, and <50% kinase inhibition activities in each kinase assay, respectively. The benzamide **1c**, which has a bromo group at a *meta* position on the aniline moiety, exhibited inhibitory

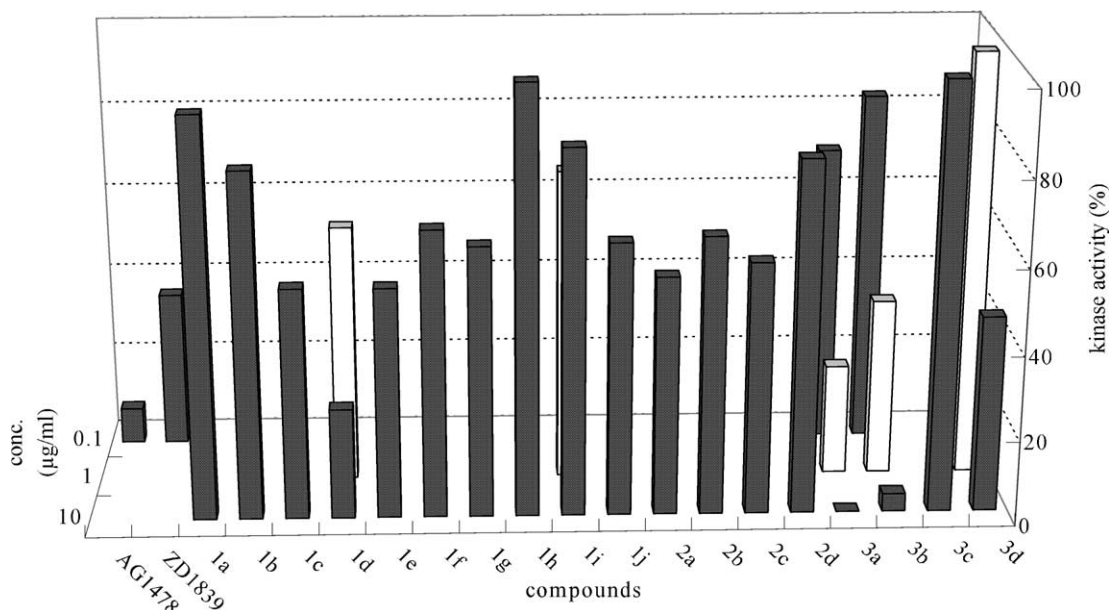


**Figure 2.** Inhibition of EGF-stimulated EGFR phosphorylation by compounds. EGFR tyrosine kinase activities are expressed as a percentage of the maximal phosphorylation induced by EGF.

activities toward EGFR and Flt-1 at a 10 µg/mL concentration. The benzamide **1d**, the benzamidine **2a**, and the cyclic benzamidine **3a** exhibited selective inhibitory activities toward EGFR at a 10 µg/mL concentration. Moreover, the cyclic benzamidine **3a** showed a high inhibition of EGFR tyrosine kinase even at a 1.0 µg/mL concentration. Although the benzamide **1j** and the benzamidine **2d** did not show the inhibition of EGFR kinase, the specific inhibition activity was observed in the case of v-Src at a 10 µg/mL concentration.

### 2.3. Molecular modeling of inhibitors in the ligand binding site of EGFR-PTK

To better understand the structure–activity relationship between the EGFR-PTK inhibitory activity and the

**Table 2.** Inhibition specificity of the compounds **1c**, **1d**, **1j**, **2a**, **2d**, and **3a**

Com- pounds	Concn (µg/ mL)	PKA	PKC	v-Src	eEF2K	EGFR	Flt-1
<b>1c</b>	10	–	–	–	–	+	+
	1	–	–	–	–	–	–
<b>1d</b>	10	–	–	–	–	+	–
	1	–	–	–	–	–	–
<b>1j</b>	10	–	–	+	–	–	–
	1	–	–	–	–	–	–
<b>2a</b>	10	–	–	–	–	+	–
	1	–	–	–	–	–	–
	0.1	–	–	–	–	–	–
<b>2d</b>	10	–	–	+	–	–	–
	1	–	–	–	–	–	–
<b>3a</b>	10	–	–	–	–	++	–
	1	–	–	–	–	+	–
	0.1	–	–	–	–	–	–

++: inhibition more than 80%, +: inhibition of 50–80%, –: inhibition under 50%.

possible binding modes of the pseudocycle **1c** and the cyclic benzamidine **3a**, we performed molecular docking experiments of **1c** and **3a** with the ligand binding site of EGFR kinase (PDB code 1M17). The protein backbone was taken from the X-ray structure of EGFR kinase domain in complex with erlotinib (Tarceva™), which has been currently studied in Phase III clinical trials as anticancer agent. Docking calculations were carried out by replacing the erlotinib with compounds **1c** and **3a**.<sup>44–46</sup> Figure 3a shows the docking mode of the benzamide **1c** overlaid with the binding conformation of erlotinib into the active site of EGFR kinase domain. Superimposition of the benzamide **1c** with the control ligand, erlotinib, shows a slightly different binding mode. Although we expected the pseudocycle formation of the benzamide **1c** through an intramolecular hydrogen bonding in the binding site of EGFR-PTK, the formation of the rotamer **1c'** would be more suitable to be positioned in the binding site according to the docking calculation, as shown in Scheme 6. A hydrogen bonding was observed between the nitrogen (N1) of the quinazoline ring and the amide nitrogen of Met-769 of the EGFR kinase domain in the crystal structure complexed with erlotinib, whereas a hydrogen bonding was observed between the amine hydrogen atom of the benzamide **1c** and the carbonyl oxygen of Met-769 in the ligand binding pocket. A little difference in the formation of hydrogen bonding between the inhibitors and the kinase domain may affect the inhibition of EGFR kinase activity. The LigScore2 scoring function gives us an index of the binding affinity of protein–ligand complexes and the higher value of the LigScore2 indicates the higher binding affinity of a protein–ligand complex.<sup>47</sup> The LigScore2 value of erlotinib was calculated as 5.61, whereas that of the benzamide **1c** was 5.05. These docking calculations also support the results obtained from the EGFR kinase assay that erlotinib possesses a higher inhibition of the EGFR kinase activity in comparison with the benzamide **1c**.

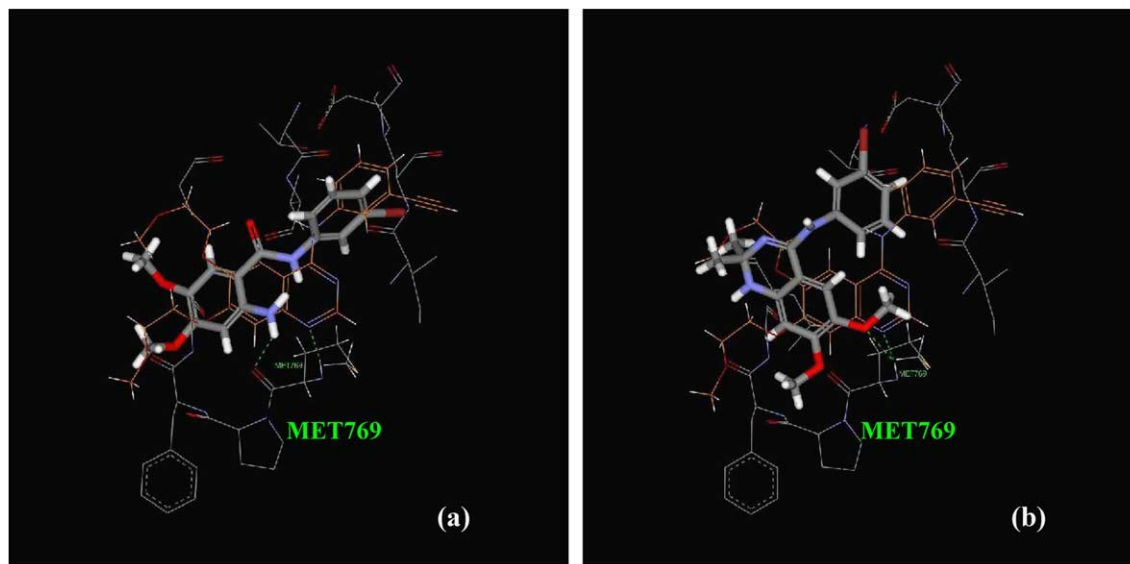
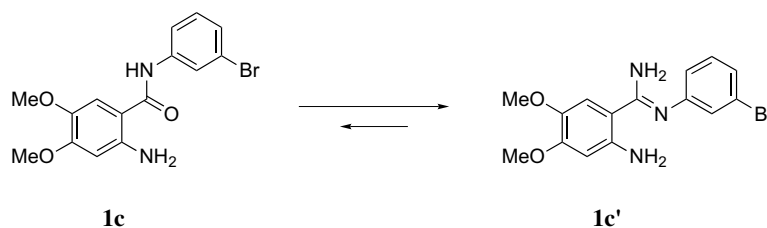


**Figure 3.** Docking modes of the benzamide **1c** (a) and the cyclic benzamidine **3a** (b) overlaid with the binding conformation of erlotinib into the active site of EGFR kinase domain. Docking model was calculated by the DS modeling based on the X-ray analysis data of EGFR-PTK with erlotinib (PDB code: 1M17).<sup>22</sup> The docked molecules are indicated by gray thick sticks and the binding orientation of erlotinib is drawn by orange sticks. Hydrogen bonds are shown as a green dotted line.



**Scheme 6.** A equilibrium between the benzamide **1c** and **1c'**.

Figure 3b shows the docking mode of the cyclic benzamidine **3a** superimposed on the binding conformation of erlotinib into the active site of EGFR kinase domain. According to the docking simulation, the cyclic benzamidine **3a** showed a quite different binding mode from erlotinib. A hydrogen bonding was observed between the methoxy oxygen on the benzene ring and the amide nitrogen of Met-769 of EGFR kinase domain and the similar hydrogen binding was observed in the crystal structure of EGFR kinase domain complexed with erlotinib. The LigScore2 value of the cyclic benzamidine **3a** was calculated as 5.10. This value indicates that the cyclic benzamidine **3a** is higher potent for the inhibition of the EGFR kinase activity in comparison with **1c**.

### 3. Conclusion

We succeeded in the synthesis of the benzamides **1** and the benzamidines **2** as the mimics of 4-anilinoquinazolines. The specific inhibitions of EGFR tyrosine kinase were observed in the benzamides **1c** and **1d**, and the benzamidine **2a**, whereas the specific inhibitions of v-Src kinase were observed in the benzamide **1j** and the benzamidine **2d** at a 10  $\mu\text{g}/\text{mL}$  concentration of compounds. The cyclic benzamidines **3a** and **3b** showed a

potent kinase inhibition of EGFR at a 1.0  $\mu\text{g}/\text{mL}$  concentration. The structure–activity relationship of the benzamide **1c** by the docking calculation revealed that the formation of the rotamer **1c'** would be more suitable to be positioned in the binding site, although the pseudocycle formation of a quinazoline ring through the intramolecular hydrogen bonding was expected. This stable formation of **1c'** resulted in the lower inhibition of EGFR tyrosine kinase in comparison with 4-anilinoquinazolines such as AG 1478 and ZD 1839. The docking simulation of the cyclic benzamidine **3a**, which showed the highest inhibition of EGFR tyrosine kinase among the compounds synthesized in this paper, revealed the possibility of the different binding mode from the benzamide **1c** or erlotinib. We believe that the current information would be very useful for designs of protein tyrosine kinase-targeted new therapeutic agents.

### 4. Experimental

#### 4.1. Chemistry

$^1\text{H}$  NMR and  $^{13}\text{C}$  NMR spectra were measured on a JEOL JNM-AL300 (300 MHz) and VARIAN UNITY-INNOVA 400 (400 MHz) spectrometers. Chemical shifts

of  $^1\text{H}$  NMR and  $^{13}\text{C}$  NMR were expressed in parts per million. IR spectra were measured on a Shimadzu FTIR-8200A Spectrometer. Analytical thin layer chromatography (TLC) was performed on a glass plates (Merck Kieselgel 60 F<sub>254</sub>, layer thickness 0.2 mm or RP-18 F<sub>254s</sub>, layer thickness 0.2 mm). Visualization was accompanied by UV light (254 nm), anisaldehyde and  $\text{KMnO}_4$ . Column chromatography was performed on silica gel (Merck Kieselgel 70–230 mesh). All reactions were carried out under argon atmosphere using standard Schlenk techniques. Most chemicals and solvents were analytical grade and used without further purification.

**4.1.1. *N*-Boc protection of 2-amino-4,5-dimethoxyanthranilic acid (4).** To a mixture of 2-amino-4,5-dimethoxybenzoic acid **4** (1.4 g, 7 mmol) in dioxane (15 mL) and water (7.5 mL) were added triethylamine (1.4 mL, 10 mmol) followed by di-*tert*-butyl dicarbonate (2.4 mL, 10 mmol). The reaction mixture was stirred at room temperature for 24 h. Solvent was removed by rotary evaporation, and 3N aqueous hydrochloric acid was added dropwise to the residue. A precipitate was obtained, collected, washed with water, and dried to provide the *N*-Boc anthranilic acid (2.0 g, >99%) as a solid;  $^1\text{H}$  NMR ( $\text{CDCl}_3$ , 400 MHz)  $\delta$  9.97 (s, 1H), 8.08 (s, 1H), 7.59 (s, 1H), 7.50 (d, 2H), 7.36 (t, 2H), 7.17 (d, 1H), 6.98 (s, 1H), 3.96 (s, 3H), 3.88 (s, 3H), 1.50 (s, 9H).  $^{13}\text{C}$  NMR ( $\text{CDCl}_3$ , 100 MHz)  $\delta$  167.2, 153.2, 152.8, 143.3, 137.3, 136.3, 129.1, 124.9, 121.1, 111.4, 109.9, 103.5, 80.3, 56.6, 56.0, 28.3.

**4.1.2. [4,5-Dimethoxy-2-cyclohexylcarbamoylphenyl]-carbamamic acid *tert*-butyl ester (6a).** To a solution of the *N*-Boc anthranilic acid (0.6 g, 2 mmol) in dry DMF (6 mL) were added EDCI (0.58 g, 3 mmol), HOBt (0.41 g, 3 mmol) and triethylamine (1.39 mL, 10 mmol). After stirring at room temperature for 24 h, cyclohexylamine (1.1 mL, 10 mmol) was added dropwise and the reaction continued for 48 h at room temperature under argon. Water was then added and the mixture stirred for 5 min. The product was then extracted with ethyl acetate. The combined organic extracts were washed with brine, dried over sodium sulfate, filtered, and the solvent removed. Purification was achieved by flash chromatography (ethyl acetate/hexane 1:5 by volume) to yield **6a** (0.59 g, 78%) as a solid:  $^1\text{H}$  NMR ( $\text{CDCl}_3$ , 400 MHz)  $\delta$  10.4 (br s, 1H), 8.07 (s, 1H), 6.85 (s, 1H), 5.98 (s, 1H), 3.94 (s, 3H), 3.90 (t,  $J = 11.2$  Hz, 1H), 3.84 (s, 3H), 2.0–1.65 (m, 5H), 1.50 (s, 9H), 1.45–1.16 (m, 5H).  $^{13}\text{C}$  NMR ( $\text{CDCl}_3$ , 400 MHz)  $\delta$  167.7, 153.2, 152.4, 143.0, 136.1, 111.0, 110.1, 103.3, 103.2, 79.9, 56.8, 56.6, 55.9, 55.8, 48.7, 48.6, 33.0, 28.3, 25.1, 24.9. IR (KBr) 3323, 2979, 1716, 1654, 1092  $\text{cm}^{-1}$ . MS (EI)  $m/z$  378 ( $\text{M}^+$ ), 278 ( $\text{M}^+ - t\text{-BuOCO}$ ), 263 ( $\text{M}^+ - t\text{-BuOCONH}$ ).

**4.1.3. [4,5-Dimethoxy-2-(1-phenyl-ethylcarbamoyl)-phenyl]-carbamamic acid *tert*-butyl ester (6b).** From the *N*-Boc anthranilic acid (0.6 g, 2 mmol), EDCI (0.6 g, 3 mmol), HOBt (0.4 g, 3 mmol), triethylamine (1.4 mL, 10 mmol),

and 1-phenylethylamine (1.3 mL, 10 mmol), a similar procedure as that described for **6a** gave **6b** (0.64 g, 79%) as a solid:  $^1\text{H}$  NMR ( $\text{CDCl}_3$ , 400 MHz)  $\delta$  10.4 (br s, 1H), 8.01 (s, 1H), 7.38–7.27 (m, 5H), 6.87 (s, 1H), 5.28 (quint,  $J = 7.0$  Hz, 1H), 3.94 (s, 3H), 3.84 (s, 3H), 1.60 (d,  $J = 7.0$  Hz, 3H), 1.50 (s, 9H). IR (KBr) 1652, 1523, 1247, 1026, 869, 815, 769  $\text{cm}^{-1}$ . HRMS (ESI) calcd for  $\text{C}_{22}\text{H}_{29}\text{N}_2\text{O}_5$ ,  $m/z$  401.2071 ( $\text{M} + \text{H}^+$ ); found,  $m/z$  401.2073.

**4.1.4. [4,5-Dimethoxy-2-(3-bromophenylcarbamoyl)-phenyl]-carbamamic acid *tert*-butyl ester (6c).** From the *N*-Boc anthranilic acid (0.6 g, 2 mmol), EDCI (0.6 g, 3 mmol), HOBt (0.4 g, 3 mmol), triethylamine (1.4 mL, 10 mmol), and 3-bromoaniline (1.1 mL, 10 mmol), a similar procedure as that described for **6a** gave the crude product of **6c**, which was used for the next *N*-Boc deprotection without further purification.

**4.1.5. [4,5-Dimethoxy-2-(3-trifluoromethyl-phenylcarbamoyl)-phenyl]-carbamamic acid *tert*-butyl ester (6d).** From the *N*-Boc anthranilic acid (0.6 g, 2 mmol), EDCI (0.6 g, 3 mmol), HOBt (0.4 g, 3 mmol), triethylamine (1.4 mL, 10 mmol), and 3-trifluoromethylaniline (1.25 mL, 10 mmol), a similar procedure as that described for **6a** gave **6d** (0.3 g, 35%) as a white solid:  $^1\text{H}$  NMR ( $\text{CDCl}_3$ , 300 MHz)  $\delta$  9.88 (s, 1H), 7.61 (dt,  $J = 2.1, 7.5$  Hz, 1H), 7.47 (s, 1H), 7.28 (s, 1H), 7.26 (d,  $J = 5.1$  Hz, 1H), 6.86 (s, 1H), 3.92 (s, 3H), 3.90 (s, 3H), 1.50 (s, 9H).  $^{13}\text{C}$  NMR ( $\text{CDCl}_3$ , 75 MHz)  $\delta$  153.1, 153.0, 143.3, 138.0, 136.3, 132.0, 131.6, 131.2, 130.8, 129.6, 123.9, 121.2, 117.8, 117.5, 111.2, 111.0, 110.0, 103.7, 80.5, 56.7, 56.1, 28.4. IR (KBr) 3321, 1685, 1517, 1163, 858, 795, 694  $\text{cm}^{-1}$ . HRMS (ESI) calcd for  $\text{C}_{21}\text{H}_{23}\text{F}_3\text{N}_2\text{O}_5$ ,  $m/z$  441.1632 ( $\text{M} + \text{H}^+$ ); found,  $m/z$  441.1633.

**4.1.6. [4,5-Dimethoxy-2-(3-methoxy-phenylcarbamoyl)-phenyl]-carbamamic acid *tert*-butyl ester (6e).** From the *N*-Boc anthranilic acid (0.6 g, 2 mmol), EDCI (0.6 g, 3 mmol), HOBt (0.4 g, 3 mmol), triethylamine (1.4 mL, 10 mmol), and 3-trifluoromethylaniline (1.25 mL, 10 mmol), a similar procedure as that described for **6a** gave **6e** (0.1 g, 18%) as a white solid:  $^1\text{H}$  NMR ( $\text{CDCl}_3$ , 300 MHz)  $\delta$  9.97 (br s, 1H), 8.07 (s, 1H), 7.80 (br s, 1H), 7.27 (t,  $J = 6.0$  Hz, 1H), 7.22 (m, 1H), 7.05 (ddd,  $J = 0.8, 0.8, 7.8$  Hz, 1H), 6.72 (dd,  $J = 2.4, 8.4$  Hz, 1H), 3.95 (s, 3H), 3.85 (s, 3H), 3.82 (s, 3H), 1.49 (s, 9H).  $^{13}\text{C}$  NMR ( $\text{CDCl}_3$ , 75 MHz)  $\delta$  167.1, 160.0, 153.1, 152.6, 143.2, 138.5, 136.1, 129.7, 113.1, 111.4, 110.4, 109.9, 106.8, 103.5, 80.3, 56.5, 56.0, 55.3, 28.4. IR (KBr) 3354, 2979, 1720, 1525, 1157, 860, 767, 685  $\text{cm}^{-1}$ . HRMS (ESI) calcd for  $\text{C}_{21}\text{H}_{29}\text{N}_2\text{O}_6$ ,  $m/z$  403.1864 ( $\text{M} + \text{H}^+$ ); found,  $m/z$  403.1866.

**4.1.7. [4,5-Dimethoxy-2-(3-chloro-4-fluorophenylcarbamoyl)-phenyl]-carbamamic acid *tert*-butyl ester (6f).** From the *N*-Boc anthranilic acid (0.6 g, 2 mmol), EDCI (0.6 g,



3 mmol), HOBT (0.4 g, 3 mmol), triethylamine (1.4 mL, 10 mmol), and 3-chloro-4-fluoroaniline (1.46 g, 10 mmol), a similar procedure as that described for **6a** gave **6f** (0.59 g, 70%) as a white solid:  $^1\text{H}$  NMR ( $\text{CDCl}_3$ , 400 MHz)  $\delta$  9.90 (br s, 1H), 8.03 (s, 1H), 7.91 (s, 1H), 7.72 (dd,  $J = 6.4, 2.8$  Hz, 1H), 7.38 (m, 1H), 7.13 (t,  $J = 8.8$  Hz, 1H), 6.96 (s, 1H), 3.93 (s, 3H), 3.82 (s, 3H), 1.50 (s, 9H).  $^{13}\text{C}$  NMR ( $\text{CDCl}_3$ , 75 MHz)  $\delta$  167.1, 156.3, 153.2, 143.4, 136.4, 134.1, 123.2, 120.7, 116.7, 116.5, 110.9, 110.1, 103.8, 80.5, 56.7, 56.1, 28.3. IR (KBr) 3323, 2980, 1716, 1655, 1092  $\text{cm}^{-1}$ . MS (EI)  $m/z$  424 ( $\text{M}^+$ ), 324 ( $\text{M}^+ - t\text{-BuOCO}$ ), 180 ( $\text{M}^+ - t\text{-BuOCO} - \text{C}_6\text{H}_3\text{ClF}$ ).

**4.1.8. 2-Amino-*N*-cyclohexyl-4,5-dimethoxy-benzamide (1a).** (A) The procedure from the carbamate **5**: A mixture of cyclohexylamine (0.3 mL, 3 mmol) and the carbamate **5** (0.6 g, 3 mmol) in DMF (5 mL) was stirred at 100 °C for 24 h. The solvent was evaporated off under reduced pressure to give a residue, which was dissolved in EtOAc and washed with saturated aqueous ammonium chloride. The solution was dried over  $\text{Na}_2\text{SO}_4$  and filtered and the solvent was evaporated off under reduced pressure to yield the crude product. The crude product was purified by column chromatography (ethyl acetate/hexane 1:5 by volume) to yield pure **1a** (0.6 g, 67%). (B) The *N*-Boc deprotection from **6a**. A solution of **6a** (0.38 g, 1 mmol) in 6:1 dichloromethane/trifluoroacetic acid (4.9 mL) was stirred at room temperature for 2 h. The solvent was evaporated in vacuo, and diethyl ether was added. The precipitate was collected, washed with ether, and dried to provide white solid **1a**:  $^1\text{H}$  NMR ( $\text{CD}_3\text{OD}$ , 300 MHz)  $\delta$  7.06 (s, 1H), 6.37 (s, 1H), 3.79 (s, 3H), 3.76 (s, 3H), 1.97–1.64 (m, 5H), 1.45–1.16 (m, 5H).  $^{13}\text{C}$  NMR ( $\text{CD}_3\text{OD}$ , 75 MHz)  $\delta$  170.3, 154.4, 146.3, 141.5, 114.0, 109.0, 101.9, 57.8, 56.1, 50.0, 33.9, 26.7, 26.6. IR (KBr) 3354, 2932, 2480, 1626, 1541, 1265, 858, 827, 771  $\text{cm}^{-1}$ . HRMS (ESI) calcd for  $\text{C}_{15}\text{H}_{22}\text{N}_2\text{O}_3$ ,  $m/z$  279.1703 ( $\text{M}+\text{H}^+$ ); found,  $m/z$  279.1704.

**4.1.9. 2-Amino-4,5-dimethoxy-*N*-(1-phenyl-ethyl)-benzamide (1b).** From compound **6b** (0.4 g, 1 mmol), a similar procedure as that described for **1a** provided the white solid **1b** (0.3 g, >99%): mp 147–149 °C;  $^1\text{H}$  NMR ( $\text{CDCl}_3$ , 400 MHz)  $\delta$  7.51 (s, 1H), 7.38–7.32 (m, 4H), 7.27 (t,  $J = 6.4$  Hz, 1H), 6.77 (s, 1H), 5.25 (t,  $J = 7.2$  Hz, 1H), 3.90 (s, 3H), 3.89 (s, 3H), 1.58 (d,  $J = 6.8$  Hz, 3H).  $^{13}\text{C}$  NMR ( $\text{CDCl}_3$ , 75 MHz)  $\delta$  165.6, 153.2, 148.9, 142.3, 142.2, 138.2, 128.5, 127.2, 126.3, 110.1, 106.9, 56.6, 56.4, 49.6, 21.1. IR (KBr) 3231, 1638, 1522, 1277, 1223, 868, 772, 704  $\text{cm}^{-1}$ . HRMS (EI) calcd for  $\text{C}_{17}\text{H}_{20}\text{N}_2\text{O}_3$ ,  $m/z$  300.1468 ( $\text{M}^+$ ); found,  $m/z$  300.1467.

**4.1.10. 2-Amino-*N*-(3-bromo-phenyl)-4,5-dimethoxy-benzamide (1c).** From compound **6c** (0.4 g, 1 mmol), a similar procedure as that described for **1a** provided white solid **1c** (0.3 g, >99%): mp >200 °C;  $^1\text{H}$  NMR ( $\text{CD}_3\text{OD}$ , 300 MHz)  $\delta$  7.99 (s, 1H), 7.61 (dt,  $J = 2.1, 7.5$  Hz, 1H), 7.47 (s, 1H), 7.28 (s, 1H), 7.26 (d,  $J = 5.1$  Hz, 1H), 6.86 (s, 1H), 3.92 (s, 3H), 3.90 (s, 3H).  $^{13}\text{C}$  NMR ( $\text{CD}_3\text{OD}$ , 75 MHz)  $\delta$  167.6, 154.2, 147.1, 141.1, 133.4, 131.1, 128.2,

125.0, 123.0, 120.7, 116.0, 113.1, 106.4, 57.3, 56.6. IR (KBr) 2940, 1664, 1587, 1205, 995, 837, 781, 721  $\text{cm}^{-1}$ . HRMS (EI) calcd for  $\text{C}_{15}\text{H}_{15}\text{N}_2\text{O}_3$ ,  $m/z$  272.1155 ( $\text{M}^+ - \text{Br}$ ); found,  $m/z$  272.1157.

**4.1.11. 2-Amino-4,5-dimethoxy-*N*-(3-trifluoromethyl-phenyl)-benzamide (1d).** From compound **6d** (0.2 g, 0.5 mmol), a similar procedure as that described for **1a** provided white solid **1d** (0.1 g, 63%): mp 158–162 °C;  $^1\text{H}$  NMR ( $\text{CD}_3\text{OD}$ , 300 MHz)  $\delta$  8.13 (s, 1H), 7.91 (d,  $J = 7.8$  Hz, 1H), 7.54 (t,  $J = 7.8$  Hz, 2H), 7.50 (s, 1H), 7.42 (d,  $J = 7.8$  Hz, 1H), 6.84 (s, 1H), 3.92 (s, 3H), 3.90 (s, 3H).  $^{13}\text{C}$  NMR ( $\text{CD}_3\text{OD}$ , 75 MHz)  $\delta$  167.8, 154.2, 147.3, 140.4, 132.1, 131.7, 130.5, 127.2, 125.3, 123.6, 121.6, 120.0, 118.7, 113.0, 57.3, 56.6. IR (KBr) 2955, 1668, 1525, 1330, 1207, 797  $\text{cm}^{-1}$ . HRMS (EI) calcd for  $\text{C}_{16}\text{H}_{15}\text{N}_2\text{O}_3$ ,  $m/z$  340.1029 ( $\text{M}^+$ ); found,  $m/z$  340.1030.

**4.1.12. 2-Amino-4,5-dimethoxy-*N*-(3-methoxy-phenyl)-benzamide (1e).** From compound **6e** (0.4 g, 1 mmol), a similar procedure as that described for **1a** provided white solid **1e** (0.3 g, >99%): mp 162–164 °C;  $^1\text{H}$  NMR ( $\text{CDCl}_3$ , 400 MHz)  $\delta$  8.18 (s, 1H), 7.21 (s, 1H), 7.17 (t,  $J = 8.0$  Hz, 1H), 7.01 (d,  $J = 8.0$  Hz, 1H), 6.90 (s, 1H), 6.67 (dd,  $J = 2.0, 8.0$  Hz, 1H), 3.92 (s, 3H), 3.81 (s, 3H), 3.75 (s, 3H).  $^{13}\text{C}$  NMR ( $\text{CDCl}_3$ , 75 MHz)  $\delta$  164.7, 159.8, 153.3, 149.1, 138.6, 138.0, 129.5, 127.0, 112.3, 110.5, 109.9, 106.9, 105.8, 56.7, 55.3. IR (KBr) 3315, 1651, 1608, 1522, 1339, 1285, 1053, 880, 762, 683  $\text{cm}^{-1}$ . HRMS (EI) calcd for  $\text{C}_{16}\text{H}_{18}\text{N}_2\text{O}_4$ ,  $m/z$  302.1261 ( $\text{M}^+$ ); found,  $m/z$  302.1263.

**4.1.13. 2-Amino-*N*-(4-chloro-3-fluoro-phenyl)-4,5-benzamide (1f).** From compound **6e** (0.4 g, 1 mmol), a similar procedure as that described for **1a** provided the white solid **1f** (0.2 g, 10%): mp 162–165 °C;  $^1\text{H}$  NMR ( $\text{CDCl}_3$ , 400 MHz)  $\delta$  8.05 (s, 1H), 7.69 (dd,  $J = 2.8, 6.6$  Hz, 1H), 7.35 (ddd,  $J = 2.6, 4.0, 9.1$  Hz, 1H), 7.07 (t,  $J = 8.8$  Hz, 1H), 6.93 (s, 1H), 6.18 (s, 1H), 3.83 (s, 3H), 3.78 (s, 3H).  $^{13}\text{C}$  NMR ( $\text{CDCl}_3$ , 75 MHz)  $\delta$  156.7, 154.1, 144.6, 141.7, 135.9, 130.2, 121.7, 116.8, 116.5, 112.5, 108.3, 101.9, 57.3, 56.1. IR (KBr) 3341, 1655, 1502, 1394, 1242, 997, 826, 769  $\text{cm}^{-1}$ . HRMS (EI) calcd for  $\text{C}_{15}\text{H}_{14}\text{ClFN}_2\text{O}_3$ ,  $m/z$  324.0671 ( $\text{M}^+$ ); found,  $m/z$  324.0673.

**4.1.14. 2-Nitro-4,5-dimethoxy-*N*-pyridin-2-yl-benzamide (10g).** A suspension of benzoic acid **9** (0.2 g, 1 mmol), 15 mL of dry  $\text{CH}_2\text{Cl}_2$ , and thionyl chloride (0.4 mL, 4 mmol) was allowed to reflux for 3 h. The solvent was removed under vacuum. To a suspension of the acid chloride in 5 mL of dry  $\text{CH}_2\text{Cl}_2$  was added 2-amino-pyridine (0.09 g, 1 mmol), and the mixture was allowed to stir at room temperature for 4 h. The solvent was removed under reduced pressure. The residue was treated with ice-water, and the pH of the slurry was adjusted to a value of 7 by adding 1 N NaOH. This solution was partitioned between EtOAc and 1 N NaOH. The layers were shaken, and the organics were separated and washed additionally with  $\text{H}_2\text{O}$ . The organic layer was

dried over Na<sub>2</sub>SO<sub>4</sub> and filtered and the solvent was removed under reduced pressure. After drying, the solid was recrystallized from the proper solvents to give **10g** (0.2 g, 50%) as a white solid: <sup>1</sup>H NMR (CDCl<sub>3</sub>, 400 MHz) δ 9.84 (s, 1H), 8.29 (d, 1H), 7.77 (d, 1H), 7.73 (t, 1H), 7.56 (s, 1H), 7.01 (s, 1H), 6.92 (q, 1H), 3.95 (s, 3H), 3.92 (s, 3H). <sup>13</sup>C NMR (CDCl<sub>3</sub>, 75 MHz) δ 165.1, 153.5, 151.6, 149.5, 146.9, 138.8, 138.6, 127.0, 119.9, 115.1, 110.1, 107.0, 56.8, 56.6. IR (KBr) 1653, 1578 1510, 1470, 1435, 1393, 1315, 1225, 1053, 875, 783 cm<sup>-1</sup>. HRMS (ESI) calcd for C<sub>14</sub>H<sub>13</sub>N<sub>3</sub>O<sub>5</sub>, *m/z* 304.0928 (M+H<sup>+</sup>); found, *m/z* 304.0927.

**4.1.15. 2-Nitro-4,5-dimethoxy-*N*-pyridin-3-yl-benzamide (10h).** From compound **9** (0.2 g, 1 mmol), a similar procedure as that described for **10g** provided the white solid **10h** (0.2 g, 67%): <sup>1</sup>H NMR (CD<sub>3</sub>OD, 400 MHz) δ 8.82 (d, 1H), 8.35 (d, 1H), 8.23 (d, 1H), 7.79 (s, 1H), 7.48 (q, 1H), 7.26 (s, 1H), 4.02 (s, 3H), 4.00 (s, 3H). <sup>13</sup>C NMR (CD<sub>3</sub>OD, 75 MHz) δ 168.0, 155.3, 151.3, 145.7, 142.2, 140.1, 137.5, 129.4, 128.0, 125.4, 111.7, 108.5, 57.3, 57.0. IR (KBr) 1661, 1508, 1281, 1227, 1055, 880, 710, 665 cm<sup>-1</sup>. HRMS (EI) calcd for C<sub>14</sub>H<sub>13</sub>N<sub>3</sub>O<sub>5</sub>, *m/z* 303.0850 (M<sup>+</sup>); found, *m/z* 303.0851.

**4.1.16. 2-Nitro-4,5-dimethoxy-*N*-pyridin-4-yl-benzamide (10i).** From compound **9** (0.2 g, 1 mmol), a similar procedure as that described for **10g** provided the white solid **10i** (0.2 g, 51%): <sup>1</sup>H NMR (CDCl<sub>3</sub>, 400 MHz) δ 8.52 (d, 2H), 7.73 (s, 1H), 7.65 (s, 1H), 7.52 (d, 2H), 6.97 (s, 1H), 3.98 (s, 6H). <sup>13</sup>C NMR (CDCl<sub>3</sub>, 75 MHz) δ 165.4, 153.8, 150.6, 149.9, 145.0, 138.4, 126.4, 113.9, 109.9, 107.1, 56.8, 56.7. IR (KBr) 1699, 1583, 1508, 1331, 1285, 1051, 876, 787 cm<sup>-1</sup>. HRMS (EI) calcd for C<sub>14</sub>H<sub>13</sub>N<sub>3</sub>O<sub>5</sub>, *m/z* 303.0850 (M<sup>+</sup>); found, *m/z* 303.0853.

**4.1.17. 2-Amino-4,5-dimethoxy-*N*-pyridin-2-yl-benzamide (1g).** A solution of nitrobenzamide **10g** (0.6 g, 2 mmol) and SnCl<sub>2</sub> (1.9 g, 10 mmol) in MeOH (90 mL) was refluxed for 3 h. After solvent removal in vacuo and digestion in CH<sub>2</sub>Cl<sub>2</sub>, saturated aqueous NaHCO<sub>3</sub> was added and the mixture was stirred for 16 h at room temperature. The mixture was then filtered through Celite and the organic layer separated. The aqueous layer was extracted with CH<sub>2</sub>Cl<sub>2</sub> and the combined organic layer were washed with water, dried (MgSO<sub>4</sub>), and evaporated in vacuo to give the amine **1g** (0.5 g, 89%) as a white solid: <sup>1</sup>H NMR (CD<sub>3</sub>OD, 400 MHz) δ 8.81 (s, 1H), 8.27 (s, 1H), 8.23 (d, *J* = 4.8 Hz, 1H), 7.70 (t, *J* = 7.2 Hz, 1H), 7.00 (q, *J* = 0.8, 4.8, 7.2 Hz, 1H), 6.96 (s, 1H), 6.19 (s, 1H), 5.51 (s, 2H), 3.84 (s, 3H), 3.78 (s, 3H). <sup>13</sup>C NMR (CD<sub>3</sub>OD, 75 MHz) δ 169.3, 155.7, 153.6, 148.8, 148.4, 141.9, 139.5, 120.6, 116.2, 113.3, 107.2, 101.8, 57.6, 56.1. IR (KBr) 3340, 2950, 1653, 1506, 1304, 1205, 1165, 999 cm<sup>-1</sup>. HRMS (EI) calcd for C<sub>14</sub>H<sub>15</sub>N<sub>3</sub>O<sub>3</sub>, *m/z* 273.1108 (M<sup>+</sup>); found, *m/z* 273.1109.

**4.1.18. 2-Amino-4,5-dimethoxy-*N*-pyridin-3-yl-benzamide (1h).** From compound **10h** (0.2 g, 1 mmol), a similar

procedure as that described for **1g** provided white solid **1h** (0.2 g, 70%): <sup>1</sup>H NMR (CDCl<sub>3</sub>, 400 MHz) δ 8.35 (d, 1H), 8.16 (d, 1H), 7.91 (s, 1H), 7.27 (q, 1H), 6.98 (s, 1H), 6.23 (s, 1H), 5.30 (s, 2H), 3.87 (s, 3H), 3.85 (s, 3H). <sup>13</sup>C NMR (CDCl<sub>3</sub>, 75 MHz) δ 170.0, 155.8, 148.4, 144.8, 143.1, 141.7, 138.0, 130.3, 125.1, 114.0, 107.2, 101.6, 57.8, 56.1. IR (KBr) 1653, 1516, 1418, 1207, 895, 795, 700 cm<sup>-1</sup>. HRMS (EI) calcd for C<sub>14</sub>H<sub>15</sub>N<sub>3</sub>O<sub>3</sub>, *m/z* 273.1108 (M<sup>+</sup>); found, *m/z* 273.1108.

**4.1.19. 2-Amino-4,5-dimethoxy-*N*-pyridin-4-yl-benzamide (1i).** From compound **10i** (0.2 g, 1 mmol), a similar procedure as that described for **1g** provided white solid **1i** (0.4 g, 73%): <sup>1</sup>H NMR (CDCl<sub>3</sub>, 400 MHz) δ 8.42 (d, 2H), 7.82 (d, 2H), 7.31 (s, 1H), 6.47 (s, 1H), 3.45 (s, 3H), 3.43 (s, 3H). <sup>13</sup>C NMR (CDCl<sub>3</sub>, 75 MHz) δ 167.3, 154.4, 150.5, 145.5, 145.4, 141.3, 114.0, 111.3, 106.8, 101.2, 57.2, 55.8. IR (KBr) 1699, 1583, 1508, 1331, 1285 cm<sup>-1</sup>. HRMS (ESI) calcd for C<sub>14</sub>H<sub>15</sub>N<sub>3</sub>O<sub>3</sub>, *m/z* 273.1108 (M<sup>+</sup>); found, *m/z* 273.1107.

**4.1.20. 6,7-Dimethoxy-2,2-dimethyl-2,3-dihydro-1*H*-quinazolin-4-one (12).** To a stirring solution of anthramide **11** (2.9 g, 15 mmol) in acetone (23 mL) was added *p*-toluenesulfonic acid monohydrate (0.01 g, 0.09 mmol), and the resulting homogeneous mixture was refluxed for 1 h. The solvent was subsequently cooled to ambient temperature and removed under reduced pressure. The resulting solid was partitioned between EtOAc and saturated aqueous NaHCO<sub>3</sub>. The layers were shaken, and the organics were separated and washed additionally with H<sub>2</sub>O. The organic layer was dried over Na<sub>2</sub>SO<sub>4</sub> and filtered and the solvent was evaporated off under reduced pressure to yield **12** (2.5 g, 71%) as a white solid: <sup>1</sup>H NMR (CD<sub>3</sub>OD, 400 MHz) δ 7.27 (s, 1H), 6.33 (s, 1H), 3.87 (s, 3H), 3.81 (s, 3H), 1.55 (s, 6H). <sup>13</sup>C NMR (CD<sub>3</sub>OD, 75 MHz) δ 166.5, 156.3, 144.8, 143.1, 111.3, 106.4, 99.0, 68.7, 57.0, 56.3, 28.9. IR (KBr) 3449, 2928, 1614, 1510, 1394, 1231, 1105, 1001 cm<sup>-1</sup>. HRMS (EI) calcd for C<sub>12</sub>H<sub>16</sub>N<sub>2</sub>O<sub>3</sub>, *m/z* 236.1155 (M<sup>+</sup>); found, *m/z* 236.1156.

**4.1.21. 6,7-Dimethoxy-2,2-dimethyl-4-methylsulfanyl-1,2-dihydro-quinazoline (13).** To a stirring solution of **12** (2.5 g, 11 mmol) in THF (22 mL) at 40 °C was added Lawesson's reagent (2.4 g, 6 mmol). The resulting mixture was heated to 80 °C for 3 h, cooled to ambient temperature and solvent removed in vacuo. The resulting foamy residue was triturated with CH<sub>2</sub>Cl<sub>2</sub>, and the solid was filtered to yield product. The filtered solid dried in a Buchner funnel overnight to afford 1.68 g of the corresponding thioamide as a yellow solid: <sup>1</sup>H NMR (CDCl<sub>3</sub>, 400 MHz) δ 7.71 (s, 1H), 6.20 (s, 1H), 3.82 (s, 3H), 3.78 (s, 3H), 1.47 (s, 6H). <sup>13</sup>C NMR (CDCl<sub>3</sub>, 75 MHz) δ 189.0, 157.2, 143.2, 141.0, 115.2, 112.7, 98.3, 68.6, 56.9.

To a stirring solution of the thioamide (2.5 g, 10 mmol) in MeOH (20 mL) was added MeI (1.87 mL, 30 mmol). The resulting dark yellow solution was stirred for 2 h,

and the solvent was removed under reduced pressure. The residue was partitioned between EtOAc and saturated aqueous NaHCO<sub>3</sub>. The layers were shaken, the organic layer separated, dried over Na<sub>2</sub>SO<sub>4</sub>, and solvent removed in vacuo. The residue was recrystallized from hexane to yield **13** (2.6 g, 98%) as a yellow solid: <sup>1</sup>H NMR (CDCl<sub>3</sub>, 400 MHz) δ 6.96 (s, 1H), 6.16 (s, 1H), 3.84 (s, 3H), 3.83 (s, 3H), 2.46 (s, 3H), 31.47 (s, 6H). <sup>13</sup>C NMR (CDCl<sub>3</sub>, 75 MHz) δ 159.2, 153.1, 141.3, 138.7, 109.1, 108.4, 98.0, 70.5, 56.6, 55.8, 29.3, 12.3. IR (KBr) 3283, 1626, 1506, 1267, 1031, 876, 837 cm<sup>-1</sup>. HRMS (EI) calcd for C<sub>13</sub>H<sub>18</sub>N<sub>2</sub>O<sub>2</sub>S, *m/z* 252.0927 (M<sup>+</sup>-CH<sub>2</sub>); found, *m/z* 252.0927.

**4.1.22. (3-Bromo-phenyl)-(6,7-dimethoxy-2,2-dimethyl-1,2-dihydro-quinazolin-4-yl)-amine (3a).** To a thiomethylether **13** (0.3 g, 1 mmol) was added 3-bromoaniline (0.5 mL, 5 mmol). The resulting homogeneous solution was heated overnight, cooled to ambient temperature, and the mixture was purified by preparative thin layer chromatography (2:1 hexane/EtOAc) to yield pure **3a** (0.2 g, 46%) as a yellow solid: <sup>1</sup>H NMR (CD<sub>3</sub>OD, 400 MHz) δ 7.48 (br s, 1H), 7.29–7.20 (m, 3H), 7.04 (d, *J* = 6.4 Hz, 1H), 6.38 (s, 1H), 3.88 (s, 3H), 3.84 (s, 3H), 1.43 (s, 6H). <sup>13</sup>C NMR (CD<sub>3</sub>OD, 75 MHz) δ 155.2, 153.3, 143.3, 143.2, 131.7, 126.7, 126.6, 123.7, 122.5, 110.6, 107.1, 99.7, 67.9, 657.3, 57.1, 56.2, 28.5. IR (KBr) 3336, 1614, 1506, 1277, 1008, 853 cm<sup>-1</sup>. HRMS (ESI) calcd for C<sub>19</sub>H<sub>20</sub>BrN<sub>3</sub>O<sub>2</sub>, *m/z* 390.0812 (M+H<sup>+</sup>); found, *m/z* 390.0812. Anal. Calcd for C<sub>19</sub>H<sub>20</sub>BrN<sub>3</sub>O<sub>2</sub>: C, 55.40; H, 5.17; N, 10.77; Br, 20.47. Found: C, 55.254; H, 5.474; N, 10.617; Br, 20.65.

**4.1.23. (3-Chloro-phenyl)-(6,7-dimethoxy-2,2-dimethyl-1,2-dihydro-quinazolin-4-yl)-amine (3b).** From a thiomethylether **13** (0.3 g, 1 mmol), a similar procedure as that described for **3a** provided a yellow solid **3b** (0.2 g, 56%): <sup>1</sup>H NMR (CD<sub>3</sub>OD, 400 MHz) δ 7.48 (s, 1H), 7.33 (t, *J* = 7.6 Hz, 1H), 7.11 (br s, 1H), 7.07 (d, *J* = 7.6 Hz, 1H), 7.01 (br s, 1H), 6.37 (s, 1H), 3.88 (s, 3H), 3.85 (s, 3H), 1.43 (s, 6H). <sup>13</sup>C NMR (CD<sub>3</sub>OD, 75 MHz) δ 155.0, 153.1, 143.2, 135.6, 131.4, 123.5, 121.9, 110.6, 107.4, 99.7, 67.9, 57.1, 56.2, 28.5. IR (KBr) 2964, 2931, 1629, 1504, 1278, 1082, 864, 827, 785. HRMS (ESI) calcd for C<sub>18</sub>H<sub>20</sub>ClN<sub>3</sub>O<sub>2</sub>, *m/z* 346.1317 (M+H<sup>+</sup>); found, *m/z* 346.1317.

**4.1.24. (6,7-Dimethoxy-2,2-dimethyl-1,2-dihydro-quinazolin-4-yl)-(3-methoxy-phenyl)-amine (3c).** From a thiomethylether **13** (0.3 g, 1 mmol), a similar procedure as that described for **3a** provided a yellow solid **3c** (0.09 g, 26%): <sup>1</sup>H NMR (CD<sub>3</sub>OD, 400 MHz) δ 7.46 (t, *J* = 8.4 Hz, 1H), 7.40 (s, 1H), 6.99 (dd, *J* = 2.4, 9.2 Hz, 1H), 6.94 (d, *J* = 3.6 Hz, 1H), 6.93 (s, 1H), 6.44 (s, 1H), 3.93 (s, 3H), 3.87 (s, 3H), 1.58 (s, 6H). <sup>13</sup>C NMR (CD<sub>3</sub>OD, 75 MHz) δ 180.4, 162.4, 154.8, 147.8, 147.3, 134.4, 131.8, 117.6, 114.4, 114.2, 113.2, 111.5, 106.7, 103.4, 67.7, 56.3, 55.9, 55.6, 27.3, 24.2. IR (KBr) 3460, 1601, 1508, 1042, 700. HRMS (ESI) calcd for

C<sub>19</sub>H<sub>23</sub>N<sub>3</sub>O<sub>3</sub>, *m/z* 342.1812 (M+H<sup>+</sup>); found, *m/z* 342.1818.

**4.1.25. (3-Chloro-4-fluoro-phenyl)-(6,7-dimethoxy-2,2-dimethyl-1,2-dihydro-quinazolin-4-yl)-amine (3d).** From a thiomethylether **13** (0.3 g, 1 mmol), a similar procedure as that described for **3a** provided a yellow solid **3d** (0.1 g, 38%): <sup>1</sup>H NMR (CD<sub>3</sub>OD, 400 MHz) δ 7.55 (s, 1H), 7.10 (t, *J* = 8.8 Hz, 1H), 7.01 (d, *J* = 4.8 Hz, 1H), 6.81 (br s, 1H), 6.19 (s, 1H), 3.88 (s, 3H), 3.86 (s, 3H), 1.47 (s, 6H). <sup>13</sup>C NMR (CD<sub>3</sub>OD, 68 MHz) δ 155.5, 153.9, 143.5, 143.5, 125.7, 123.9, 123.8, 121.8, 118.2, 117.9, 110.8, 107.2, 99.8, 98.5, 67.9, 57.1, 56.3, 28.4. IR (KBr) 3568, 3255, 1618, 1508, 1281, 1093, 781. HRMS (ESI) calcd for C<sub>19</sub>H<sub>19</sub>ClN<sub>3</sub>O<sub>2</sub>, *m/z* 364.1223 (M+H<sup>+</sup>); found, *m/z* 364.1223.

**4.1.26. 2-Amino-N-(3-bromo-phenyl)-4,5-dimethoxy-benzamidine (2a).** The acetonide **3a** (0.8 g, 2 mmol) was heated at reflux in 6 N HCl (12.5 mL) overnight and cooled to ambient temperature. The solution was evaporated at reduced pressure. The residue was taken up in isopropyl alcohol and sonicated. The solid was filtered and dried in vacuo to afford 0.2 g of **2a** as a white solid: mp 170–174 °C; <sup>1</sup>H NMR (CD<sub>3</sub>OD, 400 MHz) δ 7.85 (s, 1H), 7.71 (d, *J* = 8.4 Hz, 1H), 7.57 (m, 2H), 7.36 (s, 1H), 7.01 (s, 1H), 3.98 (s, 3H), 3.95 (s, 3H). <sup>13</sup>C NMR (CD<sub>3</sub>OD, 75 MHz) δ 163.1, 155.2, 148.6, 136.7, 133.1, 132.7, 129.5, 125.3, 124.2, 114.4, 107.4, 107.2, 57.2, 56.9. IR (KBr) 3015, 2835, 2606, 1670, 1521, 1232, 1074, 1000 cm<sup>-1</sup>. HRMS (EI) calcd for C<sub>15</sub>H<sub>16</sub>N<sub>3</sub>O<sub>2</sub>, *m/z* 349.0420 (M<sup>+</sup>); found, *m/z* 349.0422.

**4.1.27. 2-Amino-N-(3-chloro-phenyl)-4,5-dimethoxy-benzamidine (2b).** From an acetonide **3b** (0.3 g, 1 mmol), a similar procedure as that described for **2a** provided a white solid **2b** (0.2 g, 61%): mp 173–176 °C; <sup>1</sup>H NMR (CD<sub>3</sub>OD, 400 MHz) δ 7.75 (s, 1H), 7.61 (m, 3H), 7.48 (s, 1H), 7.19 (s, 1H), 4.01 (s, 3H), 3.99 (s, 3H). <sup>13</sup>C NMR (CD<sub>3</sub>OD, 75 MHz) δ 163.1, 154.7, 149.8, 136.7, 132.7, 130.4, 126.8, 125.1, 115.3, 114.6, 108.5, 57.2, 57.1. IR (KBr) 3042, 2816, 2608, 1665, 1593, 1371, 1234, 1076, 989, 868 cm<sup>-1</sup>. HRMS (EI) calcd for C<sub>15</sub>H<sub>16</sub>ClN<sub>3</sub>O<sub>2</sub>, *m/z* 305.0926 (M<sup>+</sup>); found, *m/z* 305.0928.

**4.1.28. 2-Amino-4,5-dimethoxy-N-(3-methoxy-phenyl)-benzamidine (2c).** From an acetonide **3c** (0.3 g, 1 mmol), a similar procedure as that described for **2a** provided a white solid **2c** (0.2 g, 81%): mp >200 °C; <sup>1</sup>H NMR (CD<sub>3</sub>OD, 400 MHz) δ 7.53 (t, *J* = 7.6 Hz, 1H), 7.42 (s, 1H), 7.23 (s, 1H), 7.18 (m, 2H), 7.11 (s, 2H), 4.00 (s, 3H), 3.98 (s, 3H), 3.92 (s, 3H). <sup>13</sup>C NMR (CD<sub>3</sub>OD, 75 MHz) δ 162.9, 162.2, 155.1, 147.9, 136.2, 132.0, 118.0, 115.8, 114.3, 112.8, 111.8, 106.9, 57.3, 57.0, 56.2. IR (KBr) 2835, 1655, 1524, 1234, 989, 869 cm<sup>-1</sup>. HRMS (EI) calcd for C<sub>16</sub>H<sub>19</sub>N<sub>3</sub>O<sub>3</sub>, *m/z* 301.1421 (M<sup>+</sup>); found, *m/z* 301.1424.

**4.1.29. 2-Amino-*N*-(4-chloro-3-fluoro-phenyl)-4,5-dimethoxy-benzamidine (2d).** From a acetonide **3d** (0.3 g, 1 mmol), a similar procedure as that described for **2a** provided a white solid **2d** (0.3 g, 82%): mp >200 °C; <sup>1</sup>H NMR (CD<sub>3</sub>OD, 300 MHz) δ 7.84 (br s, 1H), 7.56 (br s, 1H), 7.47 (t, *J* = 9.0 Hz, 1H), 7.39 (s, 1H), 3.95 (s, 3H), 3.93 (s, 3H). <sup>13</sup>C NMR (CD<sub>3</sub>OD, 75 MHz) δ 163.3, 160.9, 157.6, 155.0, 149.4, 131.9, 129.6, 127.6, 123.4, 119.3, 119.0, 114.4, 108.2, 57.2, 57.0. IR (KBr) 3044, 2835, 1670, 1523, 1236, 1076 cm<sup>-1</sup>. HRMS (EI) calcd for C<sub>15</sub>H<sub>15</sub>ClFN<sub>3</sub>O<sub>2</sub>, *m/z* 323.0831 (M<sup>+</sup>); found, *m/z* 323.0833.

**4.1.30. 6-Nitro-*N*-(3-bromo-phenyl)-2,3,4-trimethoxybenzamide (16).** A suspension of benzoic acid **15** (0.8 g, 3 mmol), 15 mL of dry CH<sub>2</sub>Cl<sub>2</sub>, and thionyl chloride (0.7 mL, 9 mmol) was allowed to reflux for 2 h. The solvent was removed under vacuum. To a suspension of the acid chloride in 15 mL of dry CH<sub>2</sub>Cl<sub>2</sub> was added 3-bromoaniline (0.3 mL, 3 mmol), and the mixture was allowed to stir at room temperature for 12 h. The solvent was removed under reduced pressure. The residue was treated with ice-water, and the pH of the slurry was adjusted to a value of 7 by adding 1 N NaOH. This solution was partitioned between EtOAc and 1 N NaOH. The layers were shaken, and the organics were separated and washed additionally with H<sub>2</sub>O. The organic layer was dried over Na<sub>2</sub>SO<sub>4</sub> and filtered and the solvent was removed under reduced pressure. The residue was purified by flash layer chromatography (5:1 hexane/EtOAc) to yield the pure **16** (1.0 g, 78%) as a brown solid: <sup>1</sup>H NMR (CDCl<sub>3</sub>, 300 MHz) δ 7.82 (s, 1H), 7.71 (br s, 1H), 7.51 (s, 1H), 7.48 (d, *J* = 8.0 Hz, 1H), 7.29 (d, *J* = 8.0 Hz, 1H), 7.22 (t, *J* = 8.0 Hz, 1H), 3.99 (s, 3H), 3.97 (s, 3H), 3.93 (s, 3H). <sup>13</sup>C NMR (CDCl<sub>3</sub>, 75 MHz) δ 161.7, 153.9, 150.7, 147.4, 140.9, 138.8, 130.4, 127.8, 123.2, 122.7, 121.1, 108.8, 104.2, 104.1, 62.6, 61.3, 56.6. IR (KBr) 3257, 1654, 1591, 1522, 1400, 1338, 1112, 966, 920, 775. HRMS (ESI) calcd for C<sub>16</sub>H<sub>15</sub>BrN<sub>2</sub>O<sub>6</sub>, *m/z* 411.0186 (M+H<sup>+</sup>); found, *m/z* 411.0187.

**4.1.31. 6-Amino-*N*-(3-bromo-phenyl)-2,3,4-trimethoxybenzamide (1j).** A solution of the benzamide **16** (1.0 g, 2.3 mmol) in methanol was stirred with 60 mg of 10% Pd–C under hydrogen for 4 h. The catalyst was filtered off. The solvent was then stripped off on a rotary evaporator to provide 0.9 g (>99%) of **1j** as a white solid: mp 185–187 °C; <sup>1</sup>H NMR (CDCl<sub>3</sub>, 300 MHz) δ 10.27 (s, 1H), 7.57 (d, *J* = 9.9 Hz, 2H), 7.36 (t, *J* = 7.5 Hz, 2H), 7.18 (t, *J* = 7.2 Hz, 1H), 4.06 (s, 3H), 4.01 (s, 3H), 3.90 (s, 3H). <sup>13</sup>C NMR (CDCl<sub>3</sub>, 75 MHz) δ 164.1, 156.4, 152.6, 142.1, 136.4, 128.9, 128.8, 125.3, 121.1, 110.3, 107.6, 62.5, 61.1, 57.0. IR (KBr) 2800, 1622, 1541, 1339, 1119, 806, 743 cm<sup>-1</sup>. HRMS (EI) calcd for C<sub>16</sub>H<sub>17</sub>BrN<sub>2</sub>O<sub>4</sub>, *m/z* 380.0372 (M<sup>+</sup>); found, *m/z* 380.0366.

## 4.2. Cytotoxicity

The compounds (10 mg) were dissolved in 0.1 mL of DMSO, and the resulting solution was diluted with 10%

FCS. In Falcon 3072 96-well culture plate, the cells (0.5 × 10<sup>4</sup> cells/well) were cultured on seven wells with the medium containing the compounds at various concentrations (2–2000 ppm), and incubated for 3 days at 37 °C in CO<sub>2</sub> incubator. It is known that DMSO is nontoxic at the concentration lower than 0.5%. We also confirmed by the control experiment that DMSO was nontoxic at the concentrations shown above. The medium was removed, and the cells were washed three times with PBS(–) and then dyed by crystal violet (0.4% in MeOH) for counting cells on Microplate Reader. The results are presented as the concentration of agents that resulted in 50% of the cell number of untreated cultures (IC<sub>50</sub>).

**4.2.1. EGFR tyrosine kinase assay.** For EGF receptor tyrosine kinase assay, membrane fractions were prepared from A431 cells (20 mM Hepes, pH 7.4, 0.2% Triton X-100) by the method of Hanai et al.<sup>36</sup> and the kinase assay by the method of Bertics et al.<sup>37</sup> Briefly, 15 μL of an assay mixture (20 mM Hepes, pH 7.4, 5 mM MnCl<sub>2</sub>) containing a membrane fraction of 10 μg protein and 2 μg/mL EGF and 1.0 mg/mL angiotensin II as substrate were preincubated at 25 °C for 30 min with a sample, and kinase reaction was started by adding 5 μL of [γ-<sup>32</sup>P]ATP (1 μM, 5 μCi/assay). After 15 min incubation at 0 °C, reaction was stopped with ice cold 20% trichloroacetic acid (TCA), the supernatant was spotted on P81 cellulose paper (Whatmann), washed and the radioactivities remaining were measured by scintillation counter.

**4.2.2. VEGFR tyrosine kinase assay.** VEGFR tyrosine kinase activity was measured using membrane fractions derived from Flt-1 overexpressing Tn5 cells as described.<sup>37</sup> Briefly, membrane fractions (2 μg) were incubated with kinase assay buffer containing Hepes (50 mM, pH 7.4), Triton X-100 (0.1%), MnCl<sub>2</sub> (10 mM), MgCl<sub>2</sub> (2 mM), DTT (1 mM), NaF (1 mM), Na<sub>3</sub>VO<sub>4</sub> (0.1 mM), and [γ-<sup>32</sup>P]ATP (2.5 μCi, 10 μM) at 25 °C for 10 min and the reaction was terminated by addition of SDS loading buffer. After boiling for 3 min, the reaction mixture was fractionated by SDS-PAGE (7.5% polyacrylamide gel) and bands of phosphorylated Flt-1 were visualized by autoradiography.

**4.2.3. Multiple protein kinase assay.** Kinase activities of PKA, PKC, v-Src, and eEF2K were assessed as described.<sup>38,39</sup> NIH 3T3 cells transformed with v-Src were suspended in a hypotonic buffer containing 1 mM Hepes-NaOH (pH 7.4), 5 mM MgCl<sub>2</sub>, and 25 μg/mL each of antipain, leupeptin, and pepstatin A and allowed to stand on ice for 10 min. After vigorous mixing for 1 min with a vortex mixer, the concentration of Hepes-NaOH (pH 7.4) was made equal to 20 mM. Then the lysate was centrifuged at 500g for 5 min at 4 °C to obtain the supernatant postnuclear fraction, which included protein kinases and their substrate proteins. Additions were made to the supernatant to give a final concentration of 1 mg/mL of protein/20 mM Hepes-NaOH

(pH 7.4)/10 mM MgCl<sub>2</sub>/0.1 mM Na<sub>3</sub>VO<sub>4</sub>/1 mM NaF/20 μM cAMP/100 μM CaCl<sub>2</sub>. DMSO solution of protein kinase inhibitors (3 μL) was added to 22 μL of post-nuclear fraction and the mixture was incubated for 10 min on ice. The kinase reaction was initiated by adding 5 μL of [ $\gamma$ -<sup>32</sup>P]ATP (75 μM, 10 μCi) and the mixture was incubated for 20 min at 25 °C. At the end of the reaction 10 μL of fourfold concentrated SDS-PAGE sample buffer was added to the mixture and phosphorylated protein was separated by SDS-PAGE (9% w/v gel). To detect PTK activity, the gel was further treated with NaOH (1 N) for 2 h at 55 °C. The results were visualized by autoradiography. Position of the substrate protein band of each kinase was identified according to the sensitivity to various protein kinase inhibitors or activators and phosphoamino acid analysis as previously described.

### 4.3. Docking methods

EGFR kinase domain/erlotinib complex X-ray structure (PDB code 1M17)<sup>22</sup> was taken from the Protein Data Bank. The study of complexes formed by EGFR kinase domain with **1c**, **3a**, and ATP was performed using the DS-Modeling-SBD program. Initially, hydrogen atoms were added to the protein, considering all the residues in their neutral form. Water molecules were removed and the added hydrogens were minimized while keeping all the heavy atoms fixed. The minimization followed steepest descent and conjugate gradient algorithms for interaction each using CHARMM force field in DS-Modeling-SBD. The EGFR active site was defined using the inhibitor, erlotinib [6,7-bis(2-methoxy-ethoxy)quinazoline-4-yl]-(3-ethynylphenyl)amine and included all amino acid residues within 10 Å radius from the center of the ligand. Docking was performed using the automatic calculations. The protein active site conformations for the some conformations of the ligand were retrieved for the further analysis.<sup>46</sup>

### Acknowledgements

We thank Prof. M. Shibuya (The University of Tokyo) for providing a vaculovirus vector carrying human flt-1. We also thank the Screening Committee of New Anticancer Agents supported by Grant-in-Aid for Scientific Research on Priority Area 'Cancer' from the Ministry of Education, Science, Sports, Culture and Technology, Japan for the protein kinase assay. Part of this work was supported by the Naito Foundation, Japan.

### References and notes

- Aaronson, S. A. *Science* **1991**, *254*, 1146–1152.
- Ullrich, A.; Schlessinger, J. *Cell* **1990**, *61*, 203–212.
- Elder, J. T.; Fisher, G. J.; Lindquist, P. B.; Bennett, G. L.; Pittelkow, M. R.; Coffey, R. J.; Ellingsworth, L.; Derynck, R.; Voorhees, J. J. *Science* **1989**, *243*, 811–814.
- Voldborg, B. R.; Damstrup, L.; Spang-Thomsen, M.; Poulsen, H. S. *Ann. Oncol.* **1997**, *12*, 1197–1206.
- Lawrence, D. S.; Niu, J. *Pharmacol. Ther.* **1998**, *77*, 81–114.
- Bridges, A. J. *Chem. Rev.* **2001**, *101*, 2541–2571.
- Grünwald, V.; Hidalgo, M. *J. Natl. Cancer Inst.* **2003**, *95*, 851–867.
- Fry, D. W.; Kraker, A. J.; McMichael, A.; Ambroso, L. A.; Nelson, J. M.; Leopold, W. R.; Connors, R.; Bridges, A. J. *Science* **1994**, *265*, 1093–1095.
- Ward, W. H. J.; Cook, P. N.; Slater, A. M.; Daview, H.; Holdgate, G. A.; Green, L. R. *Biochem. Pharmacol.* **1994**, *48*, 659–666.
- Rewcastle, G. W.; Denny, W. A.; Bridges, A.; Zhou, H.; Cody, D. R.; McMichael, A.; Fry, D. W. *J. Med. Chem.* **1995**, *38*, 3482–3487.
- Bridges, A.; Zhou, H.; Cody, D. R.; Rewcastle, G. W.; McMichael, A.; Showalter, H. D. H.; Fry, D. W.; Kraker, A. J.; Denny, W. A. *J. Med. Chem.* **1996**, *39*, 267–276.
- Rewcastle, G. W.; Palmer, D. B.; Thompson, A. M.; Bridges, A.; Cody, D. R.; Zhou, H.; Fry, D. W.; McMichael, A.; Denny, W. A. *J. Med. Chem.* **1996**, *39*, 1823–1835.
- Gibson, H. K.; Grundy, W.; Godfrey, A. A.; Woodburn, J. R.; Ashton, S. E.; Curry, B. J.; Scarlett, L.; Barker, A. J.; Brown, D. S. *Bioorg. Med. Chem. Lett.* **1997**, *7*, 2723–2728.
- Wissner, A.; Berger, D. M.; Boschelli, D. H.; Floyd, B., Jr; Greenberger, L. M.; Gruber, B. C.; Johnson, B. D.; Mamuya, N.; Nilakantan, R.; Reich, M. F.; Shen, R.; Tsou, H.-R.; Upeslakis, E.; Wang, Y. F.; Wu, B.; Ye, F.; Zhang, N. J. *Med. Chem.* **2000**, *43*, 3244–3256.
- Barker, A. J.; Gibson, K. H.; Grundy, W.; Godfrey, A. A.; Barlow, J. J.; Healy, M. P.; Woodburn, J. R.; Ashton, S. E.; Curry, B. J.; Scarlett, L.; Henthorn, L.; Richards, L. *Bioorg. Med. Chem. Lett.* **2001**, *11*, 1911–1914.
- Hennequin, L. F.; Thomas, A. P.; Johnstone, C.; Stokes, E. S. E.; Ple, P. A.; Johmann, J.-J. M.; Ogilvie, D. J.; Dukes, M.; Wedge, S. R.; Curwen, J. O.; Kendrew, J.; Kambert van Brempt, C. *J. Med. Chem.* **1999**, *42*, 5369–5389.
- Hennequin, L. F.; Stokes, E. S. E.; Thomas, A. P.; Johnstone, C.; Ple, P. A.; Ogilvie, D. J.; Dukes, M.; Wedge, S. R.; Kendrew, J.; Curwen, J. O. *J. Med. Chem.* **2002**, *45*, 1300–1312.
- Matsuno, K.; Ichimura, M.; Nakajima, T.; Tahara, K.; Fujiwara, S.; Kase, H.; Ushiki, J.; Giese, N. A.; Pandey, A.; Scarborough, R. M.; Lokker, N. A.; Yu, J.-C.; Irie, Y.; Tsukuda, E.; Ide, S.; Oda, S.; Nomoto, Y. *J. Med. Chem.* **2002**, *45*, 3057–3066.
- Oshero, N.; Levitzki, A. *Eur. J. Biochem.* **1994**, *225*, 1047–1053.
- Boschelli, D. H.; Ye, F. e.; Wang, Y. D.; Dutia, M.; Johnson, S. L.; Wu, B.; Miller, K.; Powell, D. W.; Yaczko, D.; Young, M.; Tischler, M.; Arndt, K.; Discifani, C.; Etienne, C.; Gibbons, J.; Grod, J.; Lucas, J.; Weber, J. M.; Boschelli, F. *J. Med. Chem.* **2001**, *44*, 3965–3977.
- Shewchuk, L.; Hassell, A.; Wisely, B.; Rocque, W.; Holmes, W.; Veal, J.; Kuyper, L. F. *J. Med. Chem.* **2000**, *43*, 133–138.
- Stamos, J.; Sliwkowski, M.; Eigenbrot, C. *J. Biol. Chem.* **2002**, *277*, 46265–46272.
- Norman, M. H.; Kelly, J. L.; Hollingsworth, E. B. *J. Med. Chem.* **1993**, *36*, 3417–3423.
- Traxler, P.; Green, J.; Mett, H.; Sequin, U.; Furet, P. J. *J. Med. Chem.* **1999**, *42*, 1018–1026.
- Minutolo, F.; Antonello, M.; Bertini, S.; Ortore, G.; Placanica, G.; Rapposelli, S.; Sheng, S.; Carlson, K. E.

- Katzenellenbogen, B. S.; Katzenellenbogen, J. A.; Macchia, M. *J. Med. Chem.* **2003**, *46*, 4032–4042.
26. Liechti, C.; Sequin, U.; Bold, G.; Furet, P.; Meyer, T.; Traxler, P. *Eur. J. Med. Chem.* **2004**, *39*, 11–26.
  27. A part of this work was published as a communication: see: Asano, T.; Yoshikawa, T.; Nakamura, H.; Uehara, Y.; Yamamoto, Y. *Bioorg. Med. Chem. Lett.* **2004**, *14*, 2299–2302.
  28. Szczepankiewicz, W.; Suwiski, J.; Bujok, R.; Gluchowski, C.; Cooper, L.; Bergbreiter, D. E.; Martin Newcomb, M. *Tetrahedron* **2000**, *56*, 9343–9349.
  29. Finch, N.; Ricca, S.; Werner, L. H.; Rodebaugh, R. *J. Org. Chem.* **1980**, *45*, 3416–3421.
  30. Manley, P. W.; Furet, P.; Bold, G.; Bruggen, J.; Mestan, J.; Meyer, T.; Schnell, C. R.; Wood, J.; Haberey, M.; Huth, A.; Kruger, M.; Menrad, A.; Ottow, E.; Seidemann, D.; Siemeister, G.; Thierauch, K.-H. *J. Med. Chem.* **2002**, *45*, 5687–5693.
  31. Grosso, J. A.; Nichols, D. E.; Kohli, J. D.; Glock, D. *J. Med. Chem.* **1982**, *25*, 703–708.
  32. Wilson, S.; Howard, P. W.; Forrow, S. M.; Hartley, J. A.; Adams, L. J.; Jenkins, T. C.; Kelland, L. R.; Thurston, D. E. *J. Med. Chem.* **1999**, *42*, 4028–4041.
  33. Larsen, S. D.; Connel, M. A.; Cudahy, M. M.; Evans, P. D.; Meglasson, M. D.; O'Sullivan, T. J.; Schostarez, H. J.; Sih, J. C.; Stevens, F. C.; Tanis, S. P.; Tegley, C. M.; Tucker, J. A.; Vaillancourt, V. A.; Vildmar, T. J.; Watt, W.; Yu, J. H. *J. Med. Chem.* **2001**, *44*, 1217–1230.
  34. Coppola, G. M.; Schuster, H. F. *J. Heterocycl. Chem.* **1989**, *26*, 957–964.
  35. Wikstrand, C. J.; McLendon, R. E.; Freidman, A. H.; Bigner, D. D. *Cancer Res.* **1997**, *57*, 4130–4140.
  36. Hanai, N.; Nores, G.; Torres-Mendez, C.; Hakomori, S. *Biochem. Biophys. Res. Commun.* **1987**, *147*, 127–134.
  37. Bertics, P. J.; Gill, G. N. *J. Biol. Chem.* **1985**, *260*, 14642–14647.
  38. Sawano, A.; Takahashi, T.; Yamaguchi, S.; Shibuya, M. *Biochem. Biophys. Res. Commun.* **1997**, *238*, 487–491.
  39. Fukazawa, H.; Li, P.-M.; Mizuno, S.; Uehara, Y. *Anal. Biochem.* **1993**, *212*, 106–110.
  40. Li, P.-M.; Fukazawa, H.; Mizuno, S.; Uehara, Y. *Anti-cancer Res.* **1993**, *13*, 1957–1964.
  41. Sasaki, S.; Hashimoto, T.; Obana, N.; Yasuda, H.; Uehara, Y.; Maeda, M. *Bioorg. Med. Chem. Lett.* **1998**, *8*, 1019–1022.
  42. Shikano, M.; Onimura, K.; Fukai, Y.; Hori, M.; Fukazawa, H.; Mizuno, S.; Yazawa, K.; Uehara, Y. *Biochem. Biophys. Res. Commun.* **1998**, *248*, 858–863.
  43. Asano, T.; Nakamura, H.; Uehara, Y.; Yamamoto, Y. *ChemBioChem* **2004**, *5*, 483–490.
  44. Wang, R.; Lu, Y.; Wang, S. *J. Med. Chem.* **2003**, *46*, 2287–2303.
  45. The 'rank-by-rank' strategy is adopted here to perform consensus scorings because the results given by the scoring functions (LigScore, PLP, PMF, and LUDI) have different units. Each scoring function involved in the given consensus-scoring scheme is applied to rank the conformations of the ligand. The final rank of a certain conformation is its average rank received from all the scoring functions. In the case of this thesis, the conformations in Figure 3 are selected from success rates of the double scoring (LigScore + LUDI). Refer to Wang et al.<sup>44</sup>
  46. Venkatachalam, C. M.; Jiang, X.; Oldfield, T.; Waldman, M. *J. Mol. Graph. Modeling* **2003**, *21*, 289–307.
  47. LigScore2 is a fast, simple scoring function for predicting protein–ligand binding affinities. The functional form of LigScore is a simple and contains only three descriptors. Eq. 1 shows the LigScore function obtained with the CFF force field using grid-based energy calculations with the improved interpolation method.<sup>44</sup>

$$pK_i = 0.517527 - 0.043650(\text{vdW\_Grid\_Soft}) + 0.143901(C + \text{pol})0.00099039(\text{Totpol}^2) \quad (1)$$

where vdW\_Grid\_Soft is the grid-based soft van der Waals energy of interaction between the ligand and the protein.  $C + \text{pol}$  is the total surface area of the ligand involved in attractive polar interactions with the protein and  $\text{Totpol}^2$  is  $(C + \text{pol})^2 + (C - \text{pol})^2$  where  $C + \text{pol}$  is the total surface area of the ligand involved in repulsive polar interactions with the protein.